Self-consistent density of states for heterostructures in strong magnetic fields

W. Xu

Department of Theoretical Physics, Research School of Physical Sciences and Engineering, The Australian National University, Canberra, Australian Capitol Territory 0200, Australia

P. Vasilopoulos

Department of Physics, Concordia University, Montreal, Quebec, Canada H3G 1M8

(Received 21 June 1993; revised manuscript received 17 June 1994)

A detailed theoretical study of the one-electron density of states (DOS) for heterostructures in a strong and transverse magnetic field B is presented for low temperatures. The Green's function for the Landau levels and the electron self-energy are calculated self-consistently including the electron interaction with background and remote impurities and with acoustic phonons through deformation and piezoelectric coupling. Transitions between Landau levels are taken into account in the self-energy. A semielliptic DOS is obtained and the Landau-level width shows a B dependence very different than $B^{1/2}$. The level shift shows considerable structure as a function of energy, magnetic field, and spin. A significant background DOS results from remote-impurity scattering for small background-impurity densities and intermediate spacer distances. The dependences on temperature, mobility, and the g factor are also investigated.

I. INTRODUCTION

Over the past two decades the investigation of magnetotransport in low-dimensional systems has been very intense.[1] A central quantity in magnetotransport studies is the density of states (DOS). In the presence of a strong-magnetic-field Landau-level quantization leads, in the absence of scattering, to a singular nature of the DOS of a two-dimensional electron gas (2DEG), with important consequences such as the quantum Hall effect, etc.

The above-mentioned singular nature of the DOS is a series of δ-function peaks centered at each Landau level (LL) with energy $E=E_N=(N+1/2)\hbar\omega_c$, $N=0, 1, 2, 3,\ldots$, where $\omega_c=eB/m^*$ is the cyclotron frequency and m^* the effective electron mass. The degeneracy of each Landau level is given by $1/2\pi l^2$ in a unit area, where $l=(\hbar/eB)^{1/2}$ is the radius of the ground cyclotron orbit. In real systems, due to scattering, inhomogeneities, etc., the Landau levels are broadened and the singularities of the DOS are damped. So far a semielliptic, a Gaussian, and a Lorentzian model have been used. An approximate calculation of the DOS in the self-consistent Born approximation (SCBA) has been carried out by Ando, Fowler, and Stern[1] for scattering with ionized impurities in a 2D system *assuming* that Landau-level mixing and the level shift are negligible and that the electron energy E is close to E_N. This resulted in a semielliptic DOS with a level width Γ_N, which for short-range scattering shows a $B^{1/2}$ dependence. Magnetization measurements on $Al_xGa_{1-x}As/GaAs$ heterostructures[2] showed roughly a $B^{1/2}$ dependence of the width Γ_N but a strong disagreement with its predicted magnitude. Later on, Gudmundsson and Gerhardts[3] proposed a statistical model for spatial inhomogeneities of the electron density in a 2DEG which simulates the electrostatic potential fluctuations. The model yielded an effective background DOS between different LL's and explained a number of experimental data.[4] In the work of Xie, Li, and Das Sarma[5] the DOS of an *ideal* 2DEG with impurity scattering was computed in the SCBA, including Landau-level mixing but no effects of phonons. The resulting DOS (the numerical DOS, without LL mixing and energy shift) showed a smoother and more realistic shape than that obtained by short-range impurity scattering. More recently, taking into account both linear and nonlinear electron-electron screening Efros, Pikus, and Burnett[6] calculated the thermodynamic DOS in a strong magnetic field . Their results showed that electron-electron screening may become important, especially when the filling factor ν is close to an integer. However, they did not make the connection of their results with an enhancement of the g factor. To study the magnetophonon resonance effect, Mori *et al.*[7] calculated the Landau-level broadening by *assuming* a semielliptic form of the DOS and taking E close to E_N. Tanatar, Singh, and MacDonald[8] have studied the effects of inelastic acoustic-phonon scattering and electron-disorder scattering self-consistently. Additional peaks were found in the DOS when the Fermi energy is away from the center of the LL's. At higher temperatures, they found some transfer of DOS from the center to the wings of the LL's. In the end, they suggested a complete self-consistent calculation of the DOS.

The brief review given above shows that more work on the DOS of quasi-two-dimensional systems is required. In this paper, we present a detailed self-consistent calculation of the DOS for a 2D system in a strong magnetic field. In contrast with previous work, we do not *assume* any particular form of the DOS and we do not *neglect* the level shift, and take into account the coupling among the LL's in the self-energy. We take into account intrasubband screening and scattering by background and remote impurities and by the deformation potential and

 ©1995 The American Physical Society

piezoelectric phonons. In addition, we consider the dependence on spin and the g factor which, to our knowledge, has not been considered. We focus on the low-temperature case and on $Al_xGa_{1-x}As/GaAs$ heterojunctions. In Sec. II, we present the method to calculate the Green's function for the Landau level and the self-energy for electrons self-consistently. In Sec. III, we discuss the situation for $Al_xGa_{1-x}As/GaAs$ heterojunctions. Our numerical results are presented and analyzed in Sec. IV and our remarks and conclusions are summarized in Sec. V.

II. SELF-CONSISTENT CALCULATION OF THE DOS

For a quasi-two-dimensional system, such as realized in AlGaAs/GaAs heterostructures, with a high-magnetic field B perpendicular to the interfaces, the Green's function for the Nth Landau level in the nth electric subband is given by

$$G_{Nn\sigma}(E)=\frac{1}{E-E_{Nn\sigma}-\mu^*-\Sigma_{Nn}(E)} ; \quad (1)$$

here, E is the electron energy, $E_{Nn\sigma}=E_N+\varepsilon_n+\sigma E_s$, $E_N=(N+\frac{1}{2})\hbar\omega_c$ is the energy of the Nth Landau level, ε_n is the energy of the nth electric subband, $\sigma=\pm1$, $E_s=g^*\mu_B B$ is the spin energy, g^* the effective spin-splitting (Landé) factor, and μ_B the Bohr magneton. Further, μ^* is the chemical potential, and the self-energy for electrons in the nth electric subband and the Nth Landau level is given by

$$\Sigma_{Nn}(E)=\Delta_{Nn}(E)-(i/2)\Gamma_{Nn}(E) . \quad (2)$$

The real part $\Delta_{Nn}(E)$ results in an energy shift and the imaginary part $\Gamma_{Nn}(E)/2$ determines the width of the broadened Landau level.

From Eqs. (1) and (2) the real and imaginary parts of the Green's function for the Landau levels are obtained as

$$\mathrm{Re}G_{Nn\sigma}(E)=\frac{E-E_{Nn\sigma}-\mu^*-\Delta_{Nn}(E)}{[E-E_{Nn\sigma}-\mu^*-\Delta_{Nn}(E)]^2+[\Gamma_{Nn}(E)/2]^2} , \quad (3a)$$

and

$$\mathrm{Im}G_{Nn\sigma}(E)=-\frac{\Gamma_{Nn}(E)/2}{[E-E_{Nn\sigma}-\mu^*-\Delta_{Nn}(E)]^2+[\Gamma_{Nn}(E)/2]^2} . \quad (3b)$$

The DOS for electrons in the Nth Landau level in the nth electric subband is given by

$$D_{Nn}(E)=-\frac{1}{2\pi^2l^2}\sum_{\sigma=\pm1}\mathrm{Im}G_{Nn\sigma}(E) . \quad (4)$$

To evaluate the Green's function, we need to know the electron's self-energy. For a quasi-two-dimensional system, the electron's self-energy is mainly determined by electron interaction with ionized impurities and phonons. Applying the lowest self-consistent Born approximation[1,5] to the impurity scattering and using the one-phonon self-energy,[9] we have

$$\Sigma_{Nn}(E)=\sum_{N',n',\mathbf{q},\sigma=\pm1}|u^i_{n'n}(\mathbf{q})|^2C_{N',N}(y)G_{N'n'\sigma}(E)$$
$$+\sum_{N',n',\mathbf{Q},\sigma=\pm1}|u^{\mathrm{ph}^+}_{n'n}(\mathbf{Q})|^2C_{N',N}(y)[N_Q+f_{N'n'\sigma}(E)]G_{N'n'\sigma}(E+\hbar\omega_Q)$$
$$+\sum_{N',n',\mathbf{Q},\sigma=\pm1}|u^{\mathrm{ph}^-}_{n'n}(\mathbf{Q})|^2C_{N',N}(y)[N_Q+1-f_{N'n'\sigma}(E)]G_{N'n'\sigma}(E-\hbar\omega_Q) , \quad (5)$$

where $y=l^2q^2/2$; $|u^i_{n'n}(\mathbf{q})|^2$ and $|u^{\mathrm{ph}^\pm}_{n'n}(\mathbf{Q})|^2$ are the squares of the electron-impurity and electron-phonon interaction matrix elements, respectively, with $\mathbf{Q}=(\mathbf{q},q_z)$ and $^{\mathrm{ph}^\pm}$ referring to the absorption (+) and emission (−) of a phonon with energy $\hbar\omega_Q$. $N_Q=1/(e^{\hbar\omega_Q/k_BT}-1)$ is the phonon occupation number, $f_{Nn\sigma}(E)=[e^{(E-E_{Nn\sigma}-\mu^*)/k_BT}+1]^{-1}$ the electron distribution function, and $C_{N,N+M}(y)=[N!/(N+M)!]y^Me^{-y}\times[L_N^M(y)]^2$ with $L_N^M(y)$ the associated Laguerre polynomial. The coupling among the different scattering processes is embedded in the Green's function. With the real and imaginary parts of Eq. (5) along with Eqs. (3), we can solve for the real and imaginary parts of the electron self-energy (and/or the Green's function for the Landau level) self-consistently. To proceed, we must specify the square of the interaction matrix elements.

For a 2DEG, the impurity scattering is mainly due to ionized impurities in the system. As for phonon scattering, it is mainly with deformation-potential acoustic (DPA), piezoelectric, and longitudinal-optical (LO) phonons. At relatively low lattice temperatures ($T<40$ K) the influence of LO phonons can be neglected. For weak electric fields, i.e., for linear responses, the electron has a small kinetic energy and the absorbed or emitted phonons have a small wave vector Q. Assuming $\hbar\omega_Q \ll k_BT$ or Γ_N is equivalent to considering the electron-phonon scattering as quasielastic for low temperatures; however, this may not always be strictly justified.[8] This approximation leads to

$$N_Q+f_{N'n'g_s}(E)\simeq k_BT/\hbar\omega_Q$$

and

$$N_Q+1-f_{N'n'g_s}(E)\simeq k_BT/\hbar\omega_Q \ . \quad (6)$$

Introducing the square of the interaction matrix element for electron scattering by DPA phonons[10] (ac), piezoelectric phonons[11] with longitudinal (pl) and transverse (pt) branches, and by impurities[12] (i) in Eq. (5), the electron's self-energy is given by

$$\Sigma_{Nn}(E)=\sum_{N',n',\sigma=\pm1}(W^{i}_{N'Nn'n}+W^{ac}_{N'Nn'n}+W^{pl}_{N'Nn'n}+W^{pt}_{N'Nn'n})G_{N'n'\sigma}(E) \ . \quad (7)$$

For impurity scattering, we have

$$W^{i}_{N'Nn'n}=2\pi\left[\frac{Ze^2}{\kappa}\right]^2\int_0^\infty\frac{dq}{q}C_{N'N}(y)\int dz_a n_i(z_a)\left[\sum_\gamma F_\gamma(q,z_a)\epsilon^{-1}_{\beta\gamma}(q)\right]^2 , \quad (8a)$$

with $\beta,\gamma=(n'n)$, κ the dielectric constant, and $F_{n'n}(q,z_a)=\langle n'|e^{-q|z-z_a|}|n\rangle$ the form factor for impurity scattering. Z is the charge number of the ionized impurity, $\epsilon_{\beta\gamma}(q)$ the matrix element of the dielectric function induced by electron-electron screening in the electric subband, and $n_i(z_a)$ the impurity distribution function. The corresponding result for DPA-phonon scattering is

$$W^{ac}_{N'Nn'n}=\frac{m^*}{\rho}\frac{E_D^2}{v_{sl}^2}\frac{\omega_c k_B T}{4\pi^2\hbar}\int_{-\infty}^{\infty}dq_z G^2_{n'n}(q_z) \ , \quad (8b)$$

with E_D the deformation-potential constant, ρ the density of the material, v_{sl} the longitudinal sound velocity, and $G^2_{n'n}(q_z)=|\langle n'|e^{-iq_z z}|n\rangle|^2$ the form factor for phonon scattering. Finally, for the longitudinal piezoelectric-phonon scattering, we have

$$W^{pl}_{N'Nn'n}=\frac{e^2e_{14}^2}{\kappa^2\rho v_{sl}^2}9k_BT\int_0^\infty dq\, q^5C_{N'N}(y)\times\int_{-\infty}^{\infty}dq_z\frac{q_z^2}{Q^8}G^2_{n'n}(q_z) \ , \quad (8c)$$

with e_{14} the piezoelectric constant, and for transverse piezoelectric-phonon scattering,

$$W^{pt}_{N'Nn'n}=\frac{e^2e_{14}^2}{\kappa^2\rho v_{st}^2}k_BT\int_0^\infty dq\, q^3C_{N'N}(y)\times\int_{-\infty}^{\infty}dq_z\frac{q^4+8q_z^4}{Q^8}G^2_{n'n}(q_z) \ , \quad (8d)$$

with v_{st} the transverse sound velocity.

In this paper, we take into account screening only for scattering by impurities. For electron-phonon scattering the influence of the dynamical screening on the transport properties (e.g., electronic mobility) is relatively weak[13] and we neglect it.

III. $Al_xGa_{1-x}As$/GaAs HETEROSTRUCTURES

In $Al_xGa_{1-x}As$/GaAs heterostructures, impurity scattering comes mainly from ionized dopants within a narrow space-charge layer in the $Al_xGa_{1-x}As$ region with a concentration N_I^r at a distance d_s (called spacer thickness) from the interface, i.e., from remote impurities, and from background-charged impurities with a concentration N_I^b in the GaAs region. In general, these impurity concentrations and distributions are not well known. We model them using

$$n_i^r(z_a)=N_I^r\delta(z_a+d_s) \text{ and } n_i^b(z_a)=N_I^b\Theta(z_a) \ . \quad (9)$$

When the electron density is less than 6×10^{11} cm^{-2}, normally only the lowest electric subband is occupied.[14] To study screening within a subband, we employ the standard random-phase approximation. Further, we make the usual triangular well approximation to model the confining potential normal to the interface and use the corresponding variational wave function.[1] Measuring energy from $E\rightarrow E-\varepsilon_0-\mu^*$, the electron's self-energy is obtained as

$$\Sigma_N(E)=\sum_{N',\sigma=\pm1}(W^{ir}_{N'N}+W^{ib}_{N'N}+W^{ac}_{N'N}+W^{pl}_{N'N}+W^{pt}_{N'N})G_{N'\sigma}(E), \quad (10)$$

where ir (ib) refers to electron scattering with remote (background) impurities and $\Sigma_N(E)=\Delta_N(E)-i\Gamma_N(E)/2$; the real and imaginary parts of the Green's function for the Landau level are given, respectively, by

$$\text{Re}G_{N\sigma}(E)=\frac{E-E_{N\sigma}-\Delta_N(E)}{[E-E_{N\sigma}-\Delta_N(E)]^2+[\Gamma_N(E)/2]^2} \quad (11a)$$

and

$$\text{Im}G_{N\sigma}(E)=-\frac{\Gamma_N(E)/2}{[E-E_{N\sigma}-\Delta_N(E)]^2+[\Gamma_N(E)/2]^2} , \quad (11b)$$

with $E_{N\sigma}=E_N+\sigma E_s$. In Eq. (10), the functional forms of $W_{N'N}$ for the different scattering processes are given by

$$W^{ir}_{N'N}=\left[\frac{e^2}{\kappa}\right]^2 2\pi N_I^r\times\int_0^\infty dx\, C_{N'N}\left[\frac{l^2b^2x^2}{2}\right]\times\frac{xe^{-2bxd_s}}{[x(1+x)^3+a_e(x)(3x^2+9x+8)]^2} , \quad (12a)$$

where $b=[(48\pi m^*e^2/\kappa\hbar^2)(N_{depl}+11n_e/32)]^{1/3}$ defines

the thickness ($=3/b$) of the triangular well, with n_e the electron density and $N_{\rm depl}$ the depletion charge density. Further,

$$a_e(x)=\frac{m^*e^2}{4\kappa\hbar^2 b}\int_0^1 \frac{dy}{Ae^{\epsilon_x(1-y^2)}+1} ,$$

with $A=[\exp(\pi\hbar^2 n_e/m^*k_BT)-1]^{-1}$ and $\epsilon_x=\hbar^2b^2x^2/8m^*k_BT$. Then

$$W_{N'N}^{ib}=\left[\frac{e^2}{\kappa}\right]^2\frac{\pi N_I^b}{2b}\times\int_0^\infty dx\, C_{N'N}\left[\frac{l^2b^2x^2}{2}\right]\times\frac{3x^5+18x^4+43x^3+48x^2+24x+2}{[x(1+x)^3+a_e(x)(3x^2+9x+8)]^2} , \tag{12b}$$

$$W_{N'N}^{\rm ac}=\frac{m^*}{\rho}\frac{E_D^2}{v_{sl}^2}\frac{3b\omega_c k_BT}{32\pi\hbar} , \tag{12c}$$

$$W_{N'N}^{\rm pl}=\frac{e^2e_{14}^2}{\kappa^2\rho v_{sl}^2}\frac{9\pi bk_BT}{16}\int_0^\infty dx\, C_{N'N}\left[\frac{l^2b^2x^2}{2}\right]\times\frac{2x^3+12x^2+6x+1}{(1+x)^4} , \tag{12d}$$

and

$$W_{N'N}^{\rm pt}=\frac{e^2e_{14}^2}{\kappa^2\rho v_{st}^2}\frac{\pi bk_BT}{16}\times\int_0^\infty dx\, C_{N'N}\left[\frac{l^2b^2x^2}{2}\right]\times\frac{6x^5+36x^4+82x^3+72x^2+78x+13}{(1+x)^6} . \tag{12e}$$

With Eqs. (10) and (11), we obtain the real and imaginary parts of the self-energy and from them the Green's function. The chemical potential can be determined self-consistently from the condition of the electron number conservation,

$$n_e=-\frac{1}{2\pi^2l^2}\sum_{N,\sigma=\pm 1}\int_{-\infty}^{\infty}dE\, f(E){\rm Im}G_{N\sigma}(E) , \tag{13}$$

with $f(E)=1/[e^{(E-\mu^*)/k_BT}+1]$ the Fermi-Dirac function.

IV. NUMERICAL RESULTS

The results of this section pertain to $Al_xGa_{1-x}As/GaAs$ heterostructures and the material parameters corresponding to GaAs are as follows: effective-mass ratio $m^*/m_e=0.0665$, static dielectric constant $\kappa=12.9$, material density $\rho=5.37$ g/cm^3, longitudinal sound velocity $v_{sl}=5.29\times10^5$ cm/s, transverse sound velocity $v_{st}=2.48\times10^5$ cm/s, the piezoelectric constant $e_{14}=1.41\times10^7$ V/cm, and the deformation-potential constant $E_D=11$ eV.

Because the ionized impurity distribution is not well known, we use the low-temperature limit of the experimental results for the mobility at zero-magnetic field μ_0 to calculate the remote-impurity concentration N_I^r with a fixed spacer d_s which normally can be determined experimentally. We take the background-impurity concentration N_I^b as a fitting parameter. For convenience, we define a parameter $\gamma_I=N_I^b/4bN_I^r$. In all calculations, we use a typical electron density $n_e=2\times10^{11}$ cm^{-2} and a typical depletion charge density $N_{\rm depl}=5\times10^{10}$ cm^{-2}. The calculation of the impurity concentration from the mobility at $T\to0$ and $B=0$ is presented in the Appendix.

To include the effect of spin into our calculation, we need to know the value of the Landé factor g^*. For bulk GaAs at low temperatures $g^*=0.44$. In $Al_xGa_{1-x}As/GaAs$ heterojunctions the g factor will be enhanced by exchange interactions.[15] An enhanced value of g^*, up to 10, has been observed and implies that the influence of spin may be important in some high-magnetic-field measurements in 2D systems. The detailed theoretical calculation of the g^* factor in a 2DEG has been summarized in Ref. 1. Here, we take g^* as a fitting parameter and for most of the calculations, we use $g^*=0.44$.

Taking into account the above remarks, we can proceed to the calculations. To solve Eqs. (10) and (11) self-consistently, we apply an iteration technique. In our calculations, the iteration is interrupted when $\max|\Gamma_N^{j+1}-\Gamma_N^j|$ and $\max|\Delta_N^{j+1}-\Delta_N^j|$, i.e., the maximum difference of Γ_N and Δ_N between two successive iteration steps j and $j+1$, are smaller than 10^{-8} meV. In all of calculations we include contributions from the lowest ten Landau levels, i.e., we take $N=0,1,\ldots,9$. Including more LL's in the calculation influences the results only for low-magnetic fields.

In Fig. 1 the Landau-level width $\Gamma_N(E)$ and the energy shift $\Delta_N(E)$, for the Landau levels $N=0$, 1, 2, 3, are plotted as a function of energy at a fixed magnetic field $B=3$ T and temperature $T=4.2$ K. The peaks of $\Gamma_N(E)$ occur when the condition $E=(M+1/2)\hbar\omega_c M=0, 1, 2,\ldots,$ is satisfied, that is, at the center of each LL. When this happens, $\Delta_N(E)$ changes sharply. Figure 1 shows that (i) for energies near the center of each Landau level the DOS is mainly determined by Γ_N, and (ii) away from these energies the DOS decreases sharply because of the increase in $|\Delta_N|$.

The DOS for the Landau levels $N=0$, 1, 2, 3 is shown in Fig. 2 as function of $E/\hbar\omega_c$ with the parameters of Fig. 1. The solid, dashed, dash-dotted, and dotted curves are the self-consistent results. It is interesting to note that though we start our calculation with a Lorentzian LL shape [see Eq. (11b)], after solving Eqs. (10) and (11) self-consistently the results show a semielliptic LL shape. From Fig. 1, we see that this is due to the self-consistency between $\Gamma_N(E)$ and $\Delta_N(E)$. The energy shift is very important in determining the LL shape. In Fig. 2, we also plot the results obtained from a semielliptic DOS (in sym-

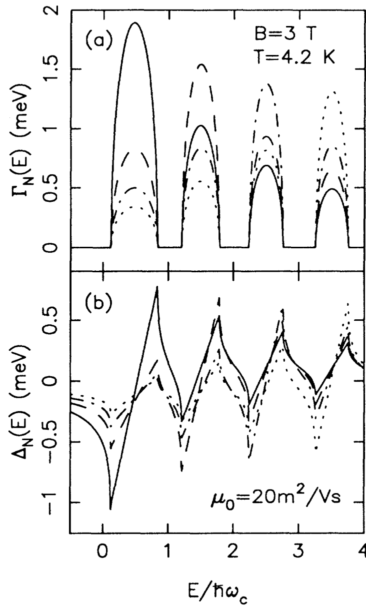

FIG. 1. (a) The Landau-level width $\Gamma_N(E)$ and (b) the energy shift $\Delta_N(E)$ as function of energy E for different Landau levels. The solid, dashed, dashed-dotted, and dotted curves correspond to $N=0$, 1, 2, and 3, respectively. The zero-field mobility μ_0, the spacer distance $d_s=100$ Å, and a fitting parameter $\gamma_I=N_I^b/4bN_I^r=0.1$ have been used to calculate the impurity concentrations. The results shown are for $g^*=0.44$ and $n_e=2\times10^{11}$ cm^{-2}. For $B=3$ T, $\hbar\omega_c=5.22$ meV. Contributions from the $N=0,\ldots 9$ Landau levels are included.

bols) using the formula

$$\mathrm{Im}G_{N\sigma}(E)=-\frac{2}{\Gamma_N(E_{N\sigma})}\times\mathrm{Re}\left[1-\left\{\frac{E-E_{N\sigma}-\Delta_N(E_{N\sigma})}{\Gamma_N(E_{N\sigma})}\right\}^2\right]^{1/2}, \tag{14}$$

where $\Gamma_N(E_{N\sigma})$ and $\Delta_N(E_{N\sigma})$ are the self-consistent results. As shown in Fig. 2 there is a very good agreement between the two results. Equation (14) is similar to the usual semielliptic DOS but we have introduced the effect of energy shift and spin. The most significant conclusion we draw from Fig. 2 is that for the more complicated calculation of magnetotransport properties, such as magnetoresistance, we can safely use the semielliptic DOS given by Eq. (14) with the self-consistent values for the LL width and the energy shift. This simplifies greatly the numerical calculation and reduces the CPU time considerably. Thus, in the following, we pay attention only to the situation where the electron energy is at the center of the LL's.

In Fig. 3, we plot $\Gamma_N(E_N\pm E_s)$ and $\Delta_N(E_N\pm E_s)$ as function of magnetic field at a fixed temperature $T=4.2$ K and mobility $\mu_0=20$ m^2/V s. The thicker linewidth curves for spin-up levels ($E=E_N+E_s$) and the thinner ones for spin-down levels ($E=E_N-E_s$); in (a) up and down results coincide. The results show that including

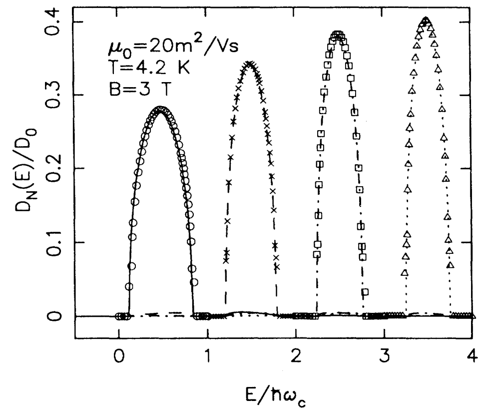

FIG. 2. The density of states as function of electron energy for different Landau levels: $N=0$ (circles and solid curve), 1 (crosses and dashed curve), 2 (squares and dashed-dotted curve), and 3 (triangles and dotted curve). The symbols are obtained by substituting the self-consistent values of $\Gamma_N(E_N\pm E_s)$ and $\Delta_N(E_N\pm E_s)$ in the semielliptic DOS given by Eq. (14). The parameters are the same as those in Fig. 1. $D_0=2m^*/\hbar^2=1.75\times10^{11}$ cm^{-2} meV^{-1}.

spin does not influence the LL width very much, but it does affect the energy shift considerably. Generally speaking, the energy shift affects the shape of the LL's, which implies that the spin effects will be reflected by the shape of magnetotransport coefficients, e.g., by the shape of Shubnikov–de Haas oscillations. Secondly, a non-$B^{1/2}$ dependence of the LL width can be observed for $B>5$ T. This is shown more clearly in Fig. 4 where we plot

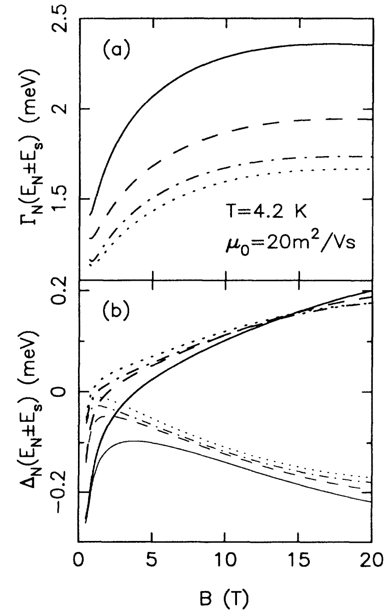

FIG. 3. (a) The Landau-level width and (b) the energy shift as a function of magnetic field for different Landau levels. The curves are marked as in Fig. 1 and the parameters are the same. The thick curves are for spin-up levels and the thin ones for the spin-down levels. In (a) spin-up and spin-down curves coincide.

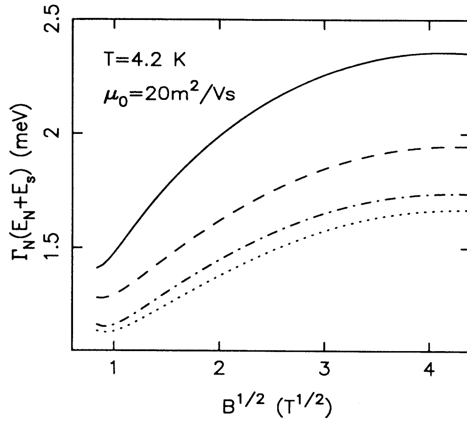

FIG. 4. Spin-up level width Γ_N as a function of $B^{1/2}$. The curves are marked as in Fig. 1. A non-$B^{1/2}$ dependence of the Landau level is evident.

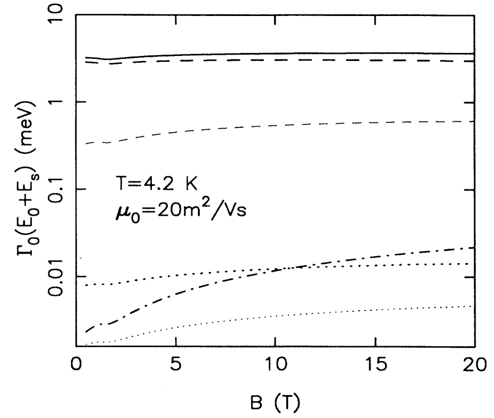

FIG. 6. Spin-up lowest-level width as a function of the magnetic field for different scattering mechanisms with the parameters of Fig. 1. The dashed curves are for scattering with remote (thick lines) and background (thin lines) impurities. The dashed-dotted curve is for scattering with acoustic phonons and the dotted curves with longitudinal (thin dots) and transverse (thick dots) piezoelectric phonons. The solid curve is the total width. Similar results are obtained for other Landau levels.

$\Gamma_N(E_N+E_s)$ as function of $B^{1/2}$. The increase of the LL width with magnetic field is slower than $B^{1/2}$, especially high-magnetic fields ($B>7$ T).

The temperature dependence of the LL width is shown in Fig. 5. The LL's are more broadened at higher temperatures because of the increase in phonon scattering. The contribution from the different scattering mechanisms to the lowest LL width, as function of the magnetic field, are shown in Fig. 6 and explained in the caption. As expected, at low temperatures and for $\gamma_I=0.1$, the main contribution to the LL broadening comes from remote-impurity scattering. Similar results are obtained for higher LL's.

In Fig. 7, we show the influence of the spin factor g^* on the LL width and the energy shift for fixed magnetic field $B=5$ T, mobility $\mu_0=20$ m^2/V s, and temperature $T=4.2$ K. The results for spin-up ($E=E_N+E_s$) and spin-down ($E=E_N-E_s$) levels are shown in thicker and thinner linewidth curves, respectively; in (a) up and down results coincide. It is interesting to note that the spin has a stronger effect on the lower-index LL's and the strongest effect can be observed for the lowest LL ($N=0$). Also, with increasing g^* first $|\Delta_N(E_N \pm E_s)|$ increases and then decreases. The maxima can be observed when g^* is around 2 corresponding to the above material parameters and experimental conditions. In fact, the spin g factor is a strong oscillatory function of the magnetic field and depends highly on the electron occupation of the Landau

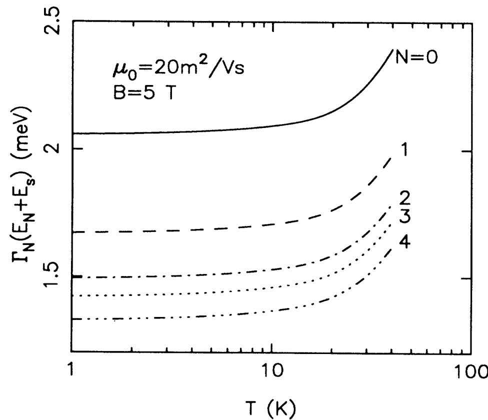

FIG. 5. The temperature dependence of the spin-up Landau-level width for fixed magnetic field. The other parameters are the same as in Fig. 1.

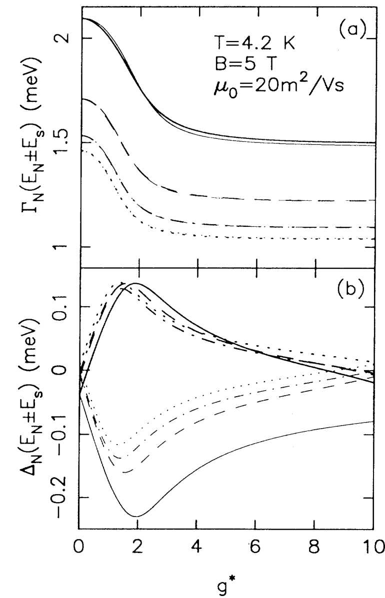

FIG. 7. (a) Landau-level width and (b) energy shift as a function of the Landé factor g^* at fixed temperature and magnetic field for different Landau levels. The curves are marked as in Fig. 3.

levels. In principle, g^* should be obtained within the self-consistent calculation of the DOS but this complicates the numerical calculation considerably and we do not attempt it.

We now focus our attention on the influence of the sample quality, connected with ionized impurity scattering, on the DOS. In Fig. 8, the LL width $\Gamma_N(E_N+E_s)$ is plotted as function of $B=0$ and $T\to 0$ mobility at a fixed magnetic field $B=5$ T and temperature $T=4.2$ K. A larger mobility corresponds to a weaker impurity scattering leading to a narrower LL width. The results show that at low temperatures, e.g., $T=4.2$ K, and for a high-quality sample, e.g., $\mu_0=20$ m^2/V s, the main contribution to the LL broadening comes from electron scattering with ionized impurities. At fixed temperature $T=4.2$ K and magnetic field $B=3$ T, and for a sample with mobility $\mu_0=20$ m^2/V s, the influence of scattering with remote and background impurities on the DOS is presented in Fig. 9 where the total density of states $D(E)=\sum_N D_N(E)$ is plotted as function of electron energy E for (a) different background-impurity concentrations (i.e., different γ_I's) at fixed spacer distance and (b) different spacer distances d_s at fixed γ_I. It can be seen that (1) a significant background DOS between the LL's can be observed for (i) small background-impurity densities $N_I^b<10^{15}$ cm^{-3}, which is satisfied in most molecular-beam epitaxy grown $Al_xGa_{1-x}As$/GaAs heterojunctions, and (ii) intermediate spacer distances $d_s\sim 100$ Å. (2) The presence of the background DOS between different LL's is a consequence of remote-impurity scattering. This is different from the result of Ref. 3, where the background DOS is induced by inhomogeneities of the 2DEG. (3) The background DOS decreases with increasing electron energy as obtained by Xie, Li, and Das Sarma.[5] (4) Our results are equivalent to those of Ref. 5, where the background DOS was induced by long-range impurity scattering. Our results and those of Ref. 5 show that scattering by short-range background impurities cannot describe the low-temperature DOS for the $Al_xGa_{1-x}As$/GaAs heterojunctions.

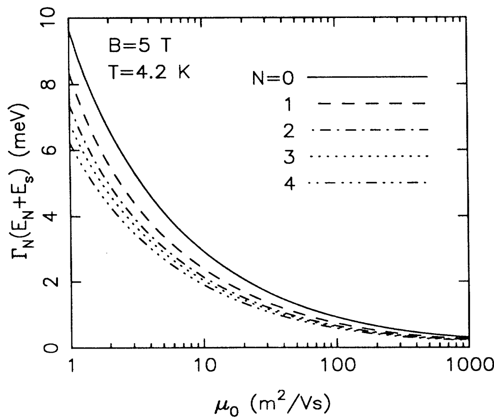

FIG. 8. Spin-up Landau-level width as function of zero-field mobility μ_0 for fixed temperature and magnetic field. The parameters are $g^*=0.44$, $d_s=100$ Å, $\gamma_I=0.01$, and $n_e=2\times 10^{11}$ cm^{-2}.

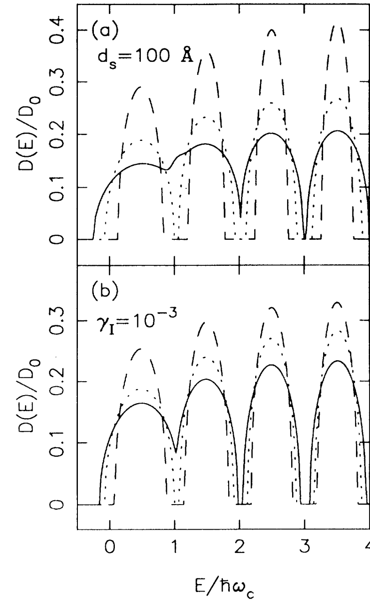

FIG. 9. Total density of states $D(E)=\sum_N D_N(E)$ as a function of electron energy E for (a) different background-impurity concentrations: $\gamma_I=1$ (dashed curve, $N_I^b=3.4\times 10^{15}$ cm^{-3}), 2.5×10^{-3} (dotted curve, $N_I^b=2.1\times 10^{15}$ cm^{-3}), and 2×10^{-4} (solid curve, $N_I^b=3.8\times 10^{14}$ cm^{-3}) at a fixed spacer distance $d_s=100$ Å; and (b) different spacer distances: $d_s=1000$ Å (dashed curve), 50 Å (dotted curve), and 100 Å (solid curve) at fixed $\gamma_I=10^{-3}$. The other parameters are $T=4.2$ K, $B=3$ T, and $\mu_0=20$ m^2/V s.

Experimentally, at low temperatures the DOS can be obtained measuring equilibrium quantities such as magnetization,[2,16] capacitance,[17] specific-heat,[2] magnetic-susceptibility,[16,18] etc. These low-temperature experiments measure the DOS at the Fermi energy, i.e., $D(\mu^*)$. In Fig. 10, we plot the chemical potential (or Fermi energy) and the total density of states $D(\mu^*)=\sum_N D_N(\mu^*)$ as a function of magnetic field for fixed temperature $T=1.2$ K and an electron density $n_e=2\times 10^{11}$ cm^{-2}. It can be seen that (1) the distribution of electron energies near the chemical potential leads to a smoother DOS (compared with the shape shown in Fig. 2). (2) The low-temperature DOS, $D(\mu^*)$, also shows a background DOS between different LL's, whereas the corresponding DOS vs electron energy (see Fig. 2) shows no background DOS. (3) The strength of the background DOS decreases with increasing magnetic field. (4) Our calculated DOS $D(\mu^*)$ has a shape very similar to the experimental result of Ref. 17, where the DOS was obtained at $T=1.3$ K by measuring the capacitance in a $Al_xGa_{1-x}As$/GaAs heterojunction with $n_e=3.6\times 10^{11}$ cm^{-2} and $\mu_0=35$ m^2/V s.

V. SUMMARY AND CONCLUSIONS

In this paper, we have studied the density of states (DOS) for electrons in a quasi-two-dimensional semiconductor system. A detailed self-consistent method was ap-

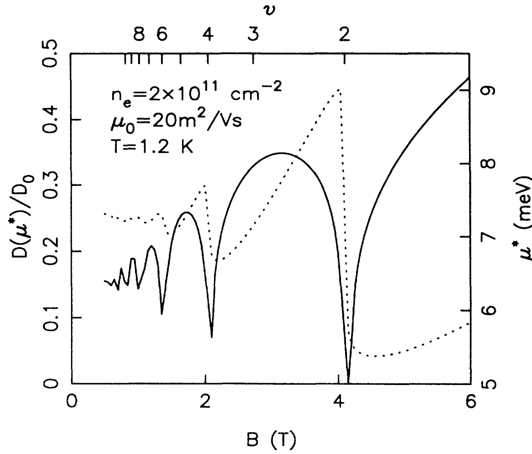

FIG. 10. Total density-of-states (solid curve) energy at the Fermi energy $D(\mu^*)=\sum_N D_N(\mu^*)$ and Fermi energy μ^* (dotted curve) as function of magnetic field at $T=1.2$ K. The other parameters are the same as in Fig. 1. $\nu=n_e h/eB$ is the filling factor.

plied to calculate the Green's function for the Landau level and the self-energy of the electrons including transitions between different LL's but considering only intrasubband screening. In our calculation, we have included the electron scattering with ionized impurities, deformation-potential acoustic phonons, and piezoelectric phonons. Also, we have taken into account the effects of spin and Landau-level shift. For $Al_xGa_{1-x}As$/GaAs heterojunctions at low temperature, we have studied the influence of electron-energy, magnetic field, different scattering processes, temperature, sample quality, and of the spin factor on the DOS. We have compared our results, supported by the experimental ones of Ref. 17, with those obtained form other theoretical models. Our conclusion are as follows.

(1) In line with previous work,[1] the width of each Landau level (LL) has a series of maxima when the electron energy is at the center of the LL's. The energy shift, previously not considered, changes sign and varies sharply when this energy is reached.

(2) A semielliptic LL shape is obtained as a consequence of the presence of the energy shift. This can be used to simplify magnetotransport calculations considerably by substituting only the self-consistent results for the LL width and energy shift, with the electron energy at the center of each LL, in Eq. (14).

(3) A non-$B^{1/2}$ dependence of the Landau-level width is observed. For low temperatures, the increase of the LL width with magnetic field is weaker than $B^{1/2}$.

(4) Increasing the temperature leads to a broader LL because of the increase in scattering by phonons. A high-quality heterojunction, i.e., one with high electronic mobility, has a narrower LL width due to the weaker impurity scattering. At low temperatures (e.g., $T=4.2$ K) and for high-quality samples the LL broadening is mainly induced by electron scattering with ionized impurities.

(5) A significant background DOS between the different LL's results from remote-impurity scattering. It can be observed for samples with low background-impurity concentration and intermediate spacer distances. Though not substantiated in our work, it may be that corrections to the SCBA lead to the appearance of a background DOS between the Landau levels as well.

(6) The effect of spin has a weak influence on the LL width in contrast with a very strong influence on the energy shift. The spin has a stronger effect on the lower-index LL's and the strongest effect is on the $N=0$ level.

(7) At low temperatures, the DOS can be smoothened by the distribution of electron energies near the Fermi energy. The background DOS decreases with increasing magnetic field. Our low-temperature DOS vs the magnetic field shows a shape very similar to that obtained experimentally in Ref. 17.

(8) The DOS of this paper is significantly different from that obtained for scattering by short-range impurities only. Inclusion of remote impurities and other scattering by acoustic and piezoelectric phonons is essential as testified by, e.g., the background DOS and the B dependence of the level width.

ACKNOWLEDGMENTS

The work of W. X. has been carried out on behalf of the Harry Triguboff AM Research Syndicate. The work of P.V. was supported by NSERC Grant No. OGPC121756. The authors are grateful to Dr. F. M. Peeters [University of Antwerp (UIA), Belgium] and Dr. D. R. Leadley (Oxford University, UK) for constructive discussions.

APPENDIX

Below, we present the formula used to calculate the impurity concentration in an Al-GaAs/GaAs heterojunction from the low temperature and zero-magnetic-field mobility. When only the lowest electric subband is occupied with electrons and in the absence of the magnetic field, the mobility in the low-temperature limit can be calculated by[19]

$$\frac{1}{\mu_0}=\frac{m^{*2}}{\pi e\hbar^3}\int_0^\pi d\theta |u_{00}^i(q)|^2(1-\cos\theta)\ , \qquad (A1)$$

where

$$|u_{00}^i(q)|^2=\left[\frac{2\pi e^2}{\kappa}\right]^2\frac{1}{q^2}\int dz_a n_i(z_a)\frac{F_{00}^2(q,z_a)}{\epsilon_{0000}^2(q)}\ , \qquad (A2)$$

with $q^2=4\pi n_e(1-\cos\theta)$ and the notations were shown in the text. We now use the variational wave function for the lowest subband,[1] the remote- and background-impurity distributions shown in Eq. (9) with $\gamma_I=N_I^b/4\pi N_I^r$, and the random-phase approximation at low temperatures, to calculate the effect of electron-electron screening. Then Eq. (A1) gives

$$\frac{1}{N_1^r} = \left[\frac{e^2}{\kappa}\right]^2 \frac{4m^{*2}\mu_0}{e\hbar^3 n_e} \int_0^1 \frac{dy\, x}{\sqrt{2-y^2}} \frac{xe^{-2bxd_s} + \gamma_I(3x^5+18x^4+43x^3+48x^2+24x+2)}{[x(1+x)^3+a_e(3x^2+9x+8)]^2} , \tag{A3}$$

with

$$x = \left[\frac{8\pi n_e}{b^2}\right]^{1/2} (1-y^2) \quad \text{and} \quad a_e = \frac{m^* e^2}{4\kappa\hbar^2 b} .$$

[1] T. Ando, A. B. Fowler, and F. Stern, Rev. Mod. Phys. **54**, 437 (1982).

[2] J. Eisenstein, *Interfaces, Quantum Wells, and Superlattices,* Vol. 179 of *NATO Advanced Study Institute, Series B: Physics* (Plenum, New York, 1987), p. 271.

[3] V. Gudmundsson and R. R. Gerhardts, Phys. Rev. B **35**, 8005 (1987).

[4] See, e.g., E. Gornik, R. Lassning, G. Strasser, H. L. Störmer, A. C. Gossard, and W. Wiegmann, Phys. Rev. Lett. **54**, 1820 (1985); E. Stahl, D. Weiss, K. von Klitzing, and K. Ploog, J. Phys. C **18**, L783 (1985).

[5] X. C. Xie, Q. P. Li, and S. Das Sarma, Phys. Rev. B **42**, 7132 (1990).

[6] A. L. Efros, F. G. Pikus, and V. G. Burnett, Solid State Commun. **84**, 91 (1992).

[7] N. Mori, H. Murata, K. Taniguchi, and C. Hamaguchi, Phys. Rev. B **38**, 7622 (1988).

[8] B. Tanatar, M. Singh, and A. H. MacDonald, Phys. Rev. B **43**, 4308 (1991).

[9] See, e.g., G. D. Mahan, *Many-Particle Physics* (Plenum, New York, 1981).

[10] P. Vogl, in *Physics of Nonlinear Transport in Semiconductors,* edited by D. K. Ferry, J. R. Barker, and C. Jacoboni (Plenum, New York, 1980), p. 75.

[11] G. D. Mahan, in *Polarons in Ionic Crystals and Polar Semiconductor,* edited by J. T. Devreese (North-Holland, Amsterdam, 1972), p. 553.

[12] X. L. Lei and C. S. Ting, J. Appl. Phys. **58**, 2270 (1985).

[13] X. L. Lei, J. Phys. C **30**, 8 (1984); W. Xu, F. M. Peeters, and J. T. Devreese, J. Phys. Condens. Matter **5**, 2307 (1993).

[14] R. Fletcher, E. Zaremba, M. D'Iorio, C. T. Foxon, and J. J. Harris, Phys. Rev. B **41**, 10 649 (1990).

[15] R. J. Nicholas, D. J. Barnes, R. G. Clark, S. R. Haynes, J. R. Mallett, A. M. Suckling, A. Usher, J. J. Harris, C. T. Foxon, and R. Willett, in *High Magnetic Fields in Semiconductor Physics II,* edited by G. Landwehr, Springer Series in Solid-State Sciences Vol. 87 (Springer-Verlag, Berlin, 1989), p. 115; B. B. Goldberg, D. Heiman, and A. Pinczuk, Surf. Sci. **229**, 137 (1990).

[16] H. L. Störmer, T. Haavasoja, V. Narayamamurti, A. C. Gossard, and W. Wiegmann, J. Vac. Sci. Technol. B **1**, 423 (1983).

[17] T. P. Smith, B. B. Godlberg, P. J. Stiles, and M. Heiblum, Phys. Rev. B **32**, 2696 (1985).

[18] E. Gornik, R. Lassning, G. Strasser, H. L. Störmer, A. C. Gossard, and W. Wiegmann, Phys. Rev. Lett. **54**, 1820 (1985).

[19] K. Hirakawa and H. Sakaki, Phys. Rev. B **33**, 8291 (1986).